最大耐力後の挙動を考慮した部材要素モデルの実験データベースに基づく精度検証 ： 鉄筋コンクリート部材およびH形鋼部材について

白, 涌滔
九州大学大学院人間環境学府空間システム専攻博士後期課程

藤井, 雅之
九州大学大学院人間環境学府空間システム専攻修士課程

江頭, 翔一
九州大学大学院人間環境学府空間システム専攻修士課程

松尾, 真太朗
九州大学大学院人間環境学研究院都市・建築学部門

他

https://doi.org/10.15017/26778

出版情報：都市・建築学研究. 22, pp.135-144, 2012-07-15. 九州大学大学院人間環境学研究院都市・建築学部門
バージョン：
権利関係：

都市・建築学研究　九州大学大学院人間環境学研究院紀要　第22号，2012年7月
J. of Architecture and Urban Design, Kyushu University, No.22, pp.135～144, July. 2012

最大耐力後の挙動を考慮した部材要素モデルの実験データベースに基づく精度検証
― 鉄筋コンクリート部材およびH形鋼部材について ―

Accuracy Verification Based on Experimental Database on Structural Member Components Covering the Post Peak behaviour
― Reinforced Concrete Members and H-shaped Steel Members ―

白　涌滔*，藤井雅之**，江頭翔一**，松尾真太朗***，河野昭彦***
Yongtao BAI*, Masayuki FUJII**, Shoichi EGASHIRA**, Shintaro MATSUO*** and Akihiko KAWANO***

In an analysis using the stress fiber discretization method, constitutive material models primarily dominate the accuracy of nonlinear behaviour for both of reinforced concrete (RC) structures and steel structures. Although various constitutive models for reinforced concrete components and steel components have been proposed, the ability of above models to capture strength and stiffness deterioration has not been fully calibrated. In this paper, comprehensive calibration and validation of the models of RC components and H-shaped steel components incorporating the strength, the ductility and the deterioration of strength and stiffness after the peaks are conducted, in order to support the prediction on the collapse resisting capacity of existing RC and steel high-rise moment resisting frame buildings. The effects of loading procedure on the strength, ductility and deterioration are investigated by comparing those of models to the experimental database. According to the calibration results, the deviation dispersion of the components under cyclic loadings is observed more widely than that of the components under uniaxial compression, since that the deterioration induced by cyclic loadings is more complex than the one of under pure uniaxial compression. Besides, the uncertainty of the post-peak deterioration of the hysteretic curves under cyclic loadings is larger than that of peak point. H-shaped steel components can be simulated more accurately than RC components for both peak point and post-peak deterioration, due to the complexity of the RC components that increase the uncertainty of the mechanical behaviour of confined concrete and steel reinforcement. The models for RC components and H-shaped steel components may have enough accuracy to predict the strength, ductility and deterioration, and further to be utilized in the collapse analysis of RC and steel high-rise moment-resisting frame buildings, respectively.

Keywords: *reinforced concrete, H-shaped steel, strength deterioration, stress-strain model, high-rise building,*
鉄筋コンクリート、H型鋼材、耐力劣化、応力―歪モデル、超高層建物

1. INTRODUCTION

Various extreme ground motions generated by great earthquakes, e.g. Hyogoken-Nanbu earthquake (1995), Tokachi earthquake (2003) and the 2011 off the Pacific Coast of Tohoku earthquake (2011), have high occurrence probability in the basin areas of Japan. Besides, ground motions generated in subduction zone or soft soil layers always incorporate long-period waves, which induce an amplification effect on the seismic responses of various high-rise buildings. Thus, the collapse potential of high-rise buildings in this study is mainly induced and accelerated by component deterioration and P-Δ effect on the basis of the theory of deformation concentration[1]. Nevertheless, one of the primary difficulties should be solved is that the

*　空間システム専攻　博士後期課程
**　空間システム専攻　修士課程
***　都市・建築学部門

deterioration model is capable to capture strength and stiffness deterioration, in order to predict the collapse capacity of structural system, with acceptable accuracy. For the existing high-rise buildings under extreme seismic excitations, the local failure (e.g. crushing in compression and cracking in tension for concrete, buckling for longitudinal steel bar) of reinforced concrete (RC) components induces strength deterioration, which could lead the structures into global failure or even collapse.

The constitutive model of confined concrete is characterized by the improvement of strength and ductility compared with plain concrete. Kent and Park[2] (1971) proposed a stress-strain model consisting of non-linear asceding branch and a linear descending branch. Popovics[3] (1973) proposed a formula to express the non-linear stress-strain relation of unconfined concrete covering from elastic to failure. Sheikh and Uzumeri (1982)[4] proposed a stress-strain model by considering the confinement effect that depends on configuration of hoop reinforcment. Mander et al.[5] (1988) studied the confinement effect of concrete by lateral ties and proposed the stress-strain model of confined concrete by adopting Popovics equation. Sargin et al.[6] studied the effects of lateral reinforcements upon the stress and deformation behavior of concrete and proposed stress-strain model of confined concrete without dimension. Sakino and Sun[7] proposed an empirical equation of the stress-strain model of confined concrete based on the basic Sargin's formula.

Preliminary studies on the deterioration models for hollow steel tubular (HST) components and concrete filled steel tubular (CFT) components are conducted by authors[8], in support of the collapse assessment on deteriorating steel moment-resisting frames and CFT moment-resisting frames. Similarly, in order to investigate the seismic performance and collapse capacity of RC high-rise moment-resisting frame structures, deteriorating stress-strain model for reinforced concrete (RC) and H-shaped steel component are also needed to be calibrated by experimental tests.

2. STRESS-STRAIN MODEL WITH DETERIORATION

The deteriorating stress-strain models of confined concrete and steel components are developed to present the strength and stiffness deterioration of various components, and further to investigate the effect of the deterioration on the seismic performance and collapse capacity of various high-rise buildings.

2.1 Deterioration model for concrete

In order to respectively evaluate the various behaviors of concrete at different phases (i.e. pre-peak behavior before concrete crush occuring, post-peak behavior after concrete crush occuring, and residual behavior after concrete crush ending), the stress-strain model of confined concrete is separated into three branches which are asceding branch, deterioration branch and residual branch. According to the method of the fiber element analysis[9]. Sectional discretization of RC components is carried out as shown in Fig. 1.

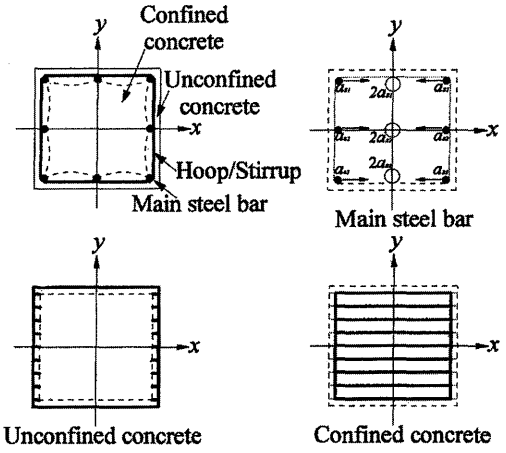

Fig. 1 Sectional discretization of RC components

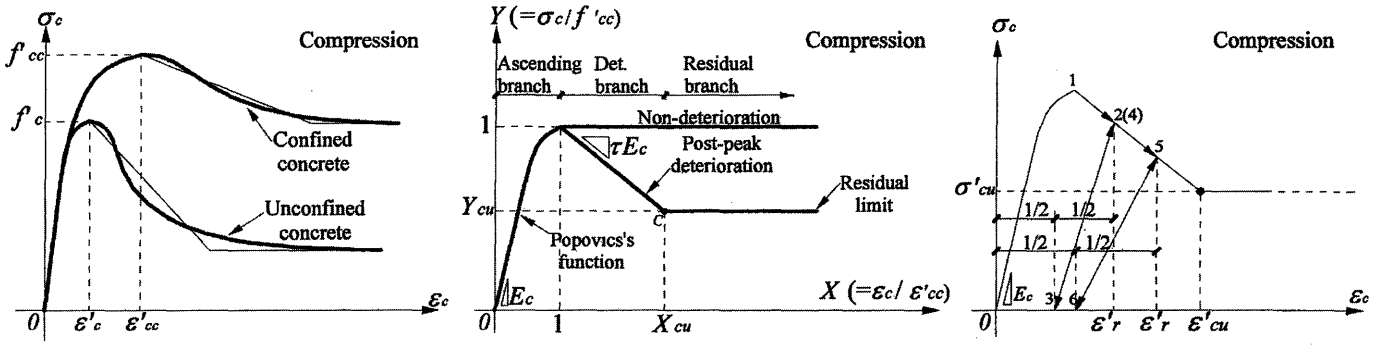

(a) Confinement effect on concrete **(b) Skeleton model** **(c) Hysteretic law**

Fig. 2 Deterioration model of concrete incorporating strength deterioration

Typical stress-strain curve of confined concrete that reflects the confinement effect are shown in Fig. 2 (a). In Fig. 2(a), the falling curve is simplfied from curved line into bilinear. Fig. 2 (b) illustrates the normalised skeleton model of confined concrete, in which, the deterioration modulus is controled by parameter τ, post-peak strength deterioration ratio is controled by parameter Y_{cu}, and also the duclity factor is controled by factor X_{cu}. These parameters are disccused in next section.

2.1.1 Ascending Branch

According to Sakino and Sun's proposal[7], the stress-strain model for concrete is normalized by the strength and corresponding strain of concrete (i.e., peak point), which is shown Table 1. The effective confinement effect factor σ_{re} is the parameter to control the confinement effects on core concrete by hoop/stirrup reinforcements. The strength and strain inprovement i.e. the peak-point (f'_{cc}, ε'_{cc}), and also the deterioration controled by parameter W which is the functions of σ_{re}.

Table 1 Parameters for concrete in RC components

	Unconfined concrete	Confined concrete
X	$\varepsilon_c / \varepsilon'_c$	$\varepsilon_c / \varepsilon'_{cc}$
Y	σ_c / f'_c	σ_c / f'_{cc}
$\varepsilon'_{cc} / \varepsilon'_c$	1	$1.0+4.7(K-1)$ $(K\leq 1.5)$ $3.4+20(K-1)$ $(K>1.5)$
$K=f'_{cc}/f'_c$	1	$1+23\sigma_{re}/f'_c$
σ_{re}	0	$\rho_w/2 \cdot \sigma_{hs}(\phi_w/C)(1-S/2D_c)$
W	$1.50-17.1\times10^{-3} f'_c$	$1.50-17.1\times10^{-3} f'_c+1.59\times\sigma_{re}^{0.5}$
V	$E_c \times \varepsilon'_{cc}/f'_{cc}$	

$f'_c = 0.85\sigma_B$

$\varepsilon'_c = 2.62 k_p^{0.25}\times10^{-3}$

$E_c = (6.90+25.72\, k_p^{0.5})\times10^3$

$k_p = f'_c / 60(\text{MPa})$

For the stress-strain relation of confined and unconfined concrete during ascending branch ($X<1$), the basic formula proposed by Popovics[3] is utilized and normalized as

$$Y = \frac{VX}{1+(V-1)X^{\frac{V}{V-1}}} \quad (X<1) \tag{2}$$

Where, V is normalized factor which is a function of E_c, σ_c and ε_c. Parameters to define the stress-strain relation in ascending branch of the concrete in RC components are expressed in Table 1. Moreover, Table 1 also shows the equations to calculate Young's modulus (E_c), the strength (f'_c) and strain (ε'_c) of unconfined concrete at peak-point, and effective confinement stress (σ_{re}).

2.1.2 Deterioration and Residual Branches

Although various nonlinear models of confined concrete has been proposed empirically, the assumption that the deterioration branch and the residual branch are represented by bilinear relation facilitate the calibration and evaluation of the strength deterioration, especially under the background that non theoretical formula is still not figured out to define the whole process of stress-strain relation for concrete yet. Thus, according to the simplified method in the companion paper[8], the deterioration and residual branches can be described by a bilinear model that shows high applicability in several studies, e.g., Park et al.[2] and Sheikh et al.[4]. In this paper, a bilinear model to define the deterioration branch and residual branch is defined by two points that are peak point (1, 1) and residual point (X_{cu}, Y_{cu}), the residual point[8] could be calculated by

$$X_{cu} = \frac{\varepsilon'_{cu}}{\varepsilon'_{cc}} = 1.96\left(\frac{V}{W}\right)^{0.88} + 4.77$$
$$Y_{cu} = \frac{\sigma'_{cu}}{f'_{cc}} = \lim_{X\to\infty}\frac{VX+(W-1)X^2}{1+(V-2)X+WX^2} = 1-\frac{1}{W} \tag{2}$$

Where, X_{cu}, represents residual strain which a function of V and W based on multiple regression, Y_{cu} represents residual strength that is controlled by parameter W, W is deterioration factor which is a function of f'_c and σ_{re}.

Fig. 2 (c) shows the hysteresis rule of concrete, that is assumed that the plastic strain after unloading is equal to a half of the strain (ε'_r) at unloading point.

2.2 Deterioration model for steel components

2.2.1 Skeleton model and Hysteretic curve

With respect to the stress-strain model of steel components, several proposals have been conducted, e.g., Ramberg-Osgood model[10] and Menegotto-Pinto (denoted as M-P model[11]), etc. The formula of M-P model is expressed by

$$\frac{\sigma}{\sigma_y} = \frac{\left(1-\frac{E_{s,\infty}}{E_s}\right)\cdot\frac{\varepsilon}{\varepsilon_y}}{\left[1+\left(\frac{\varepsilon}{\varepsilon_y}\right)^R\right]^{\frac{1}{R}}} + \left(1-\frac{E_{s,\infty}}{E_s}\right)\cdot\frac{\varepsilon}{\varepsilon_y} \tag{3}$$

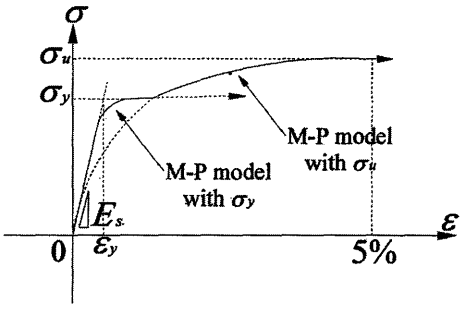

Fig. 3 Ascending branch of steel component

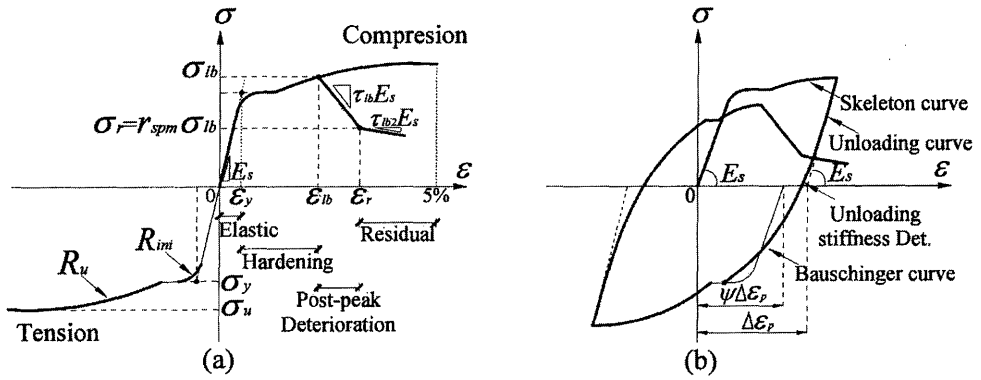

(a) Skeleton model **(b) Hysteretic rules**

Fig. 4 Deterioration model for steel component

In this paper, two M-P skeleton curves respectively controlled by the ultimate strength and yield strength are combined together to clearly describe the yield point elongation and stress hardening after steel components achieve their yield strength, which is shown in Fig. 3.

Local buckling of sectional steel and buckling of steel bar under bending or axial loading induce the above steel components occur post-peak strength deterioration, as shown in Fig. 4(a). Moreover, the residual stress branch of steel components starts from the ending of post-peak strength deterioration. Thus, the skeleton model for hysteretic curve can be confirmed by basic curve combined by two M-P model as illustrated in Fig. 3, and with deterioration and residual branches as shown in Fig. 4(a).

According to the proposal of Akiyama and Kato[12), 13)], the cyclic hysteretic curves should be divided into three portions which respectively are a part of skeleton curve, the unloading elastic curve, and Bauschinger curve. According to Ohi's proposal[14)], the skeleton curve is moved to be connected with unloading and Bauschinger curve on each hysteresis, due to unloading stiffness deterioration. The moving ratio for a part of skeleton curve, as shown in Fig. 4 (b), is based on the parameter ψ which is the ratio of moving stress value ($\psi\Delta\varepsilon_p$) to plastic stress ($\Delta\varepsilon_p$) after unloading. Realistic value of ψ is considered between 0~1, in this study, ψ is assumed to be equal to 0.8.

The point where the residual stress begins is obtained by

$$\begin{aligned}\sigma_r &= r_{spm}\cdot\sigma_{lb}\\ \varepsilon_r &= \frac{(r_{spm}-1)\sigma_{lb}}{\tau_{lb}E_s}+\varepsilon_{lb}\end{aligned} \tag{4}$$

The bilinear curve for deterioration and residual branches of steel bars are defined by

$$\begin{cases}\sigma=(\varepsilon_r-\varepsilon)\tau_{lb}E_s+\sigma_{lb} & (\varepsilon_{lb}\le\varepsilon<\varepsilon_r)\\ \sigma=\sigma_r & (\varepsilon_r\le\varepsilon)\end{cases} \tag{5}$$

Therefore, the basic backbone model that incorporates deterioration for steel components could be confirmed.

2.2.2 H-shaped steel component

The strain where local buckling of H-shaped steel component occurs is calculated by the proposal of Yamada et al.[15)], formulae are shown in Table 2, in which, strength deterioration is controlled by width-thickness ratio of flange B/T_f and web $(D-2T_f)/T_w$, and yield strength of steel σ_y. On the basis of statistical data of steel material (-0.0025~-0.0075), the second deterioration modulus τ_{lb2} for residual branch is modified into τ_{lb2}=-0.003, in order to fit test results.

Table 2 stress-strain model of H-shaped steel and steel bar

Parameter	H-shaped steel	Steel bar
α_w	$\alpha_w=[(D-2T_f)/T_w]^2\times\varepsilon_y$	-
α_f	$\alpha_f=[B/T_f]^2\times\varepsilon_y$	-
$\varepsilon_{lb}(\varepsilon_{bu})$	$\max\left[\frac{0.18}{\alpha_f}+\frac{2.6}{\alpha_w}+0.3,\ \frac{0.5}{\alpha_f}+\frac{5.7}{\alpha_w}-4.0\right]\cdot\varepsilon_y$	$\varepsilon_c'+f_1(S/B)\cdot f_2(p_w\cdot\sigma_{wy})\cdot f_3(S\cdot L)\cdot f_4(\sigma_B)\cdot f_5(\sigma_{hs})$
r_{spm}	$r_{spm}=-0.062\alpha_w-0.56\alpha_f+0.98$	$\frac{1}{\sqrt{1+0.005\lambda^2}}$
τ_{lb}	$-0.0046\alpha_w^{\ 2}-0.57\alpha_f^{\ 2}-0.0005$	$100\varepsilon_y\left(\frac{1}{\sqrt{1+0.005\lambda^2}}-1\right)$
τ_{lb2}	$\tau_{lb2}=-0.003$	$\tau_{lb2}=-0.005$

2.2.3 Deterioration of main steel bar

The formula on the strain where buckling of main steel bars occurs is proposed by Nakatsuka[16], which is

$$\varepsilon_{bu} = \varepsilon_c' + f_1(S/B)\cdot f_2(p_w\cdot\sigma_{wy})\cdot f_3(S\cdot L)\cdot f_4(\sigma_B)\cdot f_5(\sigma_{hs}) \quad (6)$$

Where, in Eq. (6), ε'_c is derived from Table 1.

Residual strength ratio (r_{spm}) is based on an assumption that the residual stress is equal to the stress where 1% strain occurs[17]. Post-peak deterioration is calculated by the two points of peak point (σ_{lb}, ε_{lb}) and residual point (σ_r, ε_r), based on the assumption that $\varepsilon_r=\varepsilon_{lb}+0.01$.

3. CALIBRARTION

FEM program[9] is applied to carry out the elasto-plastic analysis of the structural components under various loading procedures. Geometric nonlinearities are considered using an updated Lagrangean formula with a local coordinate axis for each element, which moves along with the element within the global coordinate axis system. The element stiffness was evaluated by the means of Gaussian numerical integrals using three Gaussian points (sections). The stiffness of cross sections was numerically integrated by dividing the section into a number of layers referred to as stress fibers. Finally, accurate nonlinear constitutive relations were then applied to these fibers to define the mechanical behavior of each member.

To support collapse assessment of high-rise frames (i.e. reinforced moment-resisting frame and also steel moment-resisting frame), validation and calibration of the deterioration models for RC and H-shaped steel components are needed to be conducted, on the basis of a database of RC and H-shaped steel component tests. Regarding with the reason of strength and stiffness deterioration of structural components, local failure of various components is mainly induced by compression and bending moment loadings under monotonic and cyclic loadings.

In this section, calibration of deterioration model is conducted separately by various loading conditions as shown in Fig. 5, in which, the longitudinal definition of structural element modeling is based on an assumption that the length of plastic region at the fixed ending of components where the plastic hinges form is assumed to be a constant value that is equal to the cross-section width (B) of components. Correspondingly, elastic region is also divided by cross section width (B) of components. Calibration method is based on the comparisons of peak point (i.e., strength, deformation at the peak-point) and deterioration stiffness (τ) between test results and analytical results. Fig. 6 shows the calibration methodology of specimens under monotonic loadings (axial load (Type 1), monotonic horizontal loading with constant axial load (Type 2)).

3.1 RC components

Various recent conducted tests[18)~26)] on rectangular RC specimens are referred, in which, properties of these specimens are shown as the Table 3. Regarding with the specimen under axial loading, the peak point indicates the compressive stress capacity and the strain at compressive strength, and the strength deterioration is belonged to post-peak deterioration. The relation of calibration results to deterioration parameter for RC component (hoop/stirrup reinforcement ratio p_w) is calculated and illustrated in Fig. 7. Mean value and standard deviation of the calibrated test/analysis ratio of the peak point and post peak deterioration are also presented in Fig. 7, where, peak point (axial force N, axial deformation Δ) is predicted with higher accuracy than that of post-peak deterioration. This indicates that the uncertainty of post peak deterioration is more complex to be captured. Fortunately, calibration of post peak deterioration (τ_t/τ_a) in Fig. 7, is within an acceptable deviation based on engineering demand.

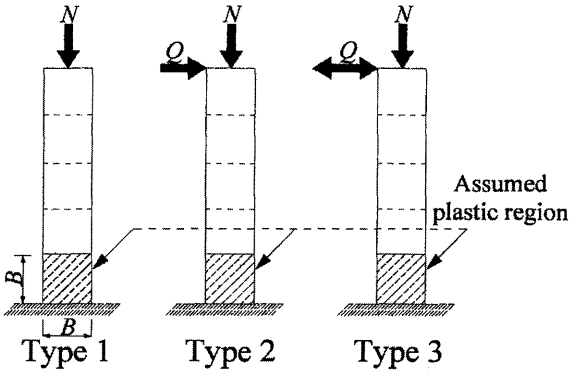

Fig. 5 Varied loading procedures of specimens

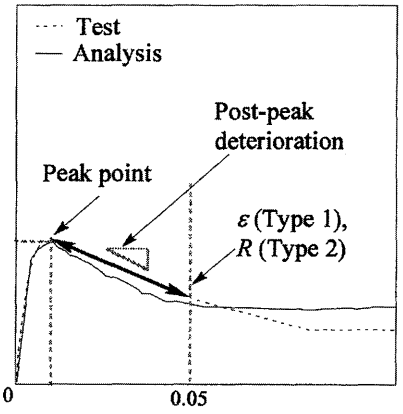

Fig. 6 Calibration methodology of the specimens subjected to loading procedures (Type 1, 2)

Table 3 Geometric and material properties of RC specimens

Researcher	Suzuki et al.[18]	Kato et al.[19]	Endo[20]	Sakino et al.[21]	Watson[22]	Gill[23]	Atalay and Penzien[24]	Soesianawati, Park and Priestley[25]	Tanaka and Park[26]
Number of specimen	3	28	5	3	3	3	10	4	4
Section (mm)	210×210	150×150	200×200	250×250	400×400	550×550	305×305	400×400	400×400/ 550×550
σ_B (N/mm^2)	32.9	24.5～91.7	17.6	83.6～94.3	40	21.4~41.4	29.1~33.3	40~46.5	25.6/32.0
n (=N/N_y)	-	-	0.15, 0.36	0.20～0.45	0.3, 0.5	0.21~0.42	0.094~0.278	0.1/0.3	0.1/0.2
σ_{hs} (N/mm^2)	334	332～1354	326	1018	255~388	275	363~392	255/364	325/333
Spacing S (mm)	20～100	30, 60	50～200	30, 60	80	75/80	76/127	78~94	80/90/110
Loading procedure	Type1	Type1	Type3	Type3	Type3	Type3	Type3	Type3	Type3

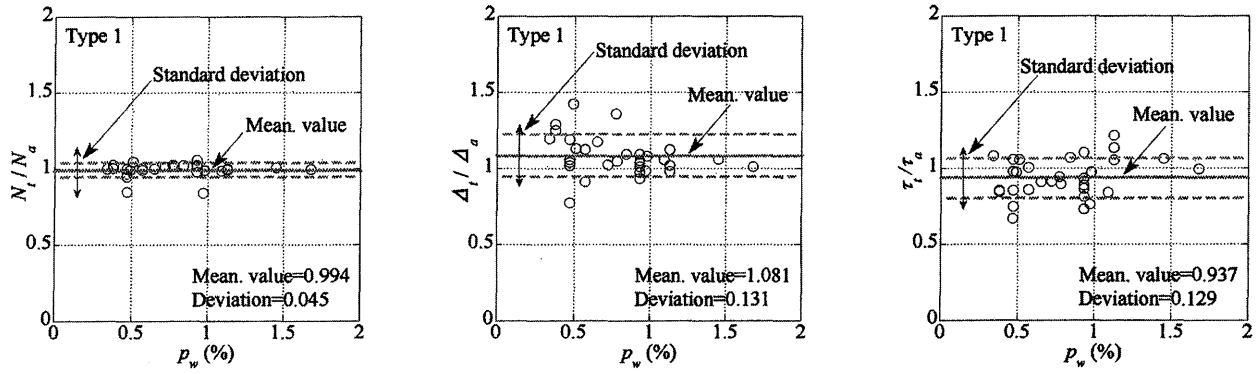

Fig. 7 Calibration of RC specimens subjected to axial loading (Type 1)

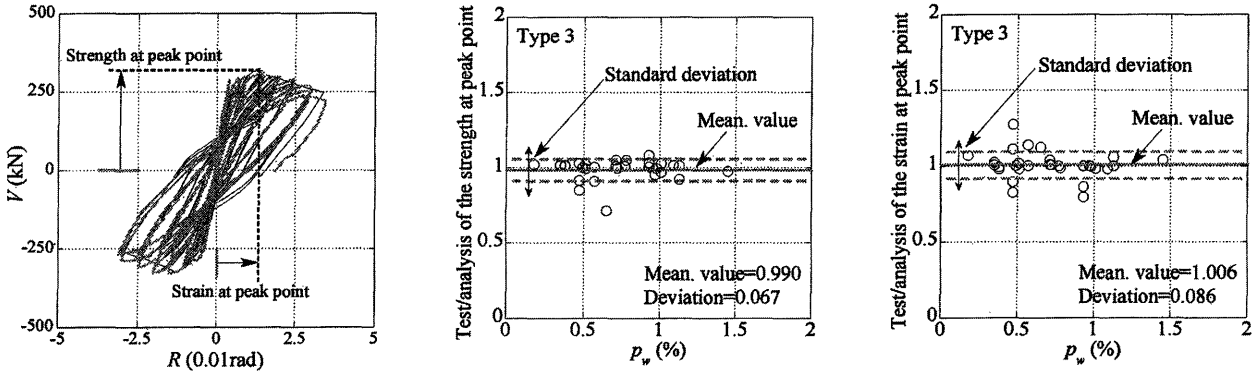

(a) Comparison methodology **(b) Strength at peak-point** **(c) Strain at peak-point**

Fig. 8 Peak-point calibration of the RC specimens subjected to cyclic loadings (Type 3)

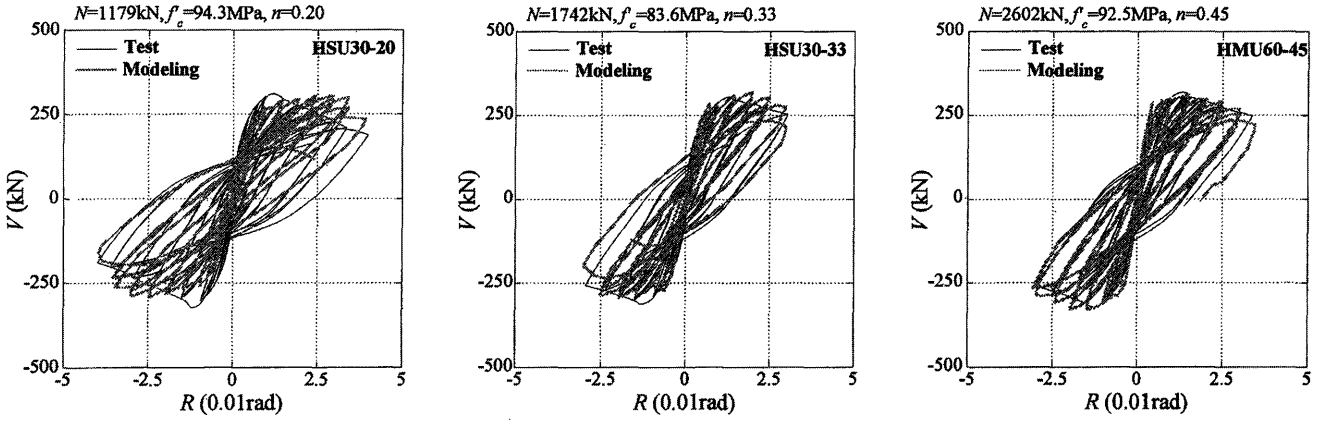

Fig. 9 Cyclic deterioration of RC specimens under cyclic loadings (Type 3)

Fig. 8 illustrates the post-peak calibration results of the RC specimens under cyclic loading with constant axial force (Type 3), based on a comparison methodology as shown in Fig. 8 (a). Furthermore, Fig. 9 gives a typical comparisons of cyclic deterioration of RC specimens with different axial load ratios (n=0.20, 0.33, 0.45). The uncertainty of steel bar and concrete materials contribute to the difficulties on predicting the strength and stiffness deterioration of RC components under complex loading histories.

3.2 H-shaped steel component

H-shaped steel component is widely applied as girder in existing high-rise steel moment-resisting frames. Therefore, validation and calibration of deterioration model for H-shaped steel components is also needed to be conducted. Methods for the calibration of existing tests[27)~31)] on H-shaped steel components are similar to the one that used for RC components. Geometric and material properties of H-shaped steel components are shown in Table 4.

As shown in Table 4, various loading procedures (i.e. uni-axial loading, monotonic or cyclic loadings with constant axial loading) of test for H-shaped steel components are simulated. Comprehensive accuracy assessment of the deterioration model is carried out by summarizing test/analysis ratio of calibration parameters against the width-thickness ratio (D/T_w), which are respectively shown in Fig. 10. Parameters of peak point and post-peak deterioration show different deviations as seen in Fig. 10, especially for the calibration ratio of post-peak deterioration, the dispersion of test/analysis ratio shows wider distribution than that at the peak point.

Table 4 Parameters of calibrated H-shaped steel specimens

Researchers	Specimen numbers	D (mm)	B (mm)	D/T_w	B/T_f	σ_y (N/mm^2)	n ($=N/N_y$)	Loading procedures
Yamada et al. [27)]	19	157~291	168~264	14.8~29.7	14.0~22.0	356~499	-	Type1
Suzuki et al.[28)]	8	150	150	22.0	16.7	291~526	-	Type1
Mukai et al.[29)]	10	138~258	108~324	20.0~40.0	12.0~36.0	300	-	Type1
Mitani[30)]	7	100~137	76~100	20.3~39.0	12.4~22.2	300~456	0.30~0.60	Type2
	5	100~136	99~100	26.6~39.1	15.2~22.1	300~320	0.30, 0.60	Type3
Matsui et al.[31)]	12	150	150	22.0, 23.0	16.7, 25.0	292~378	0.10~0.60	Type3

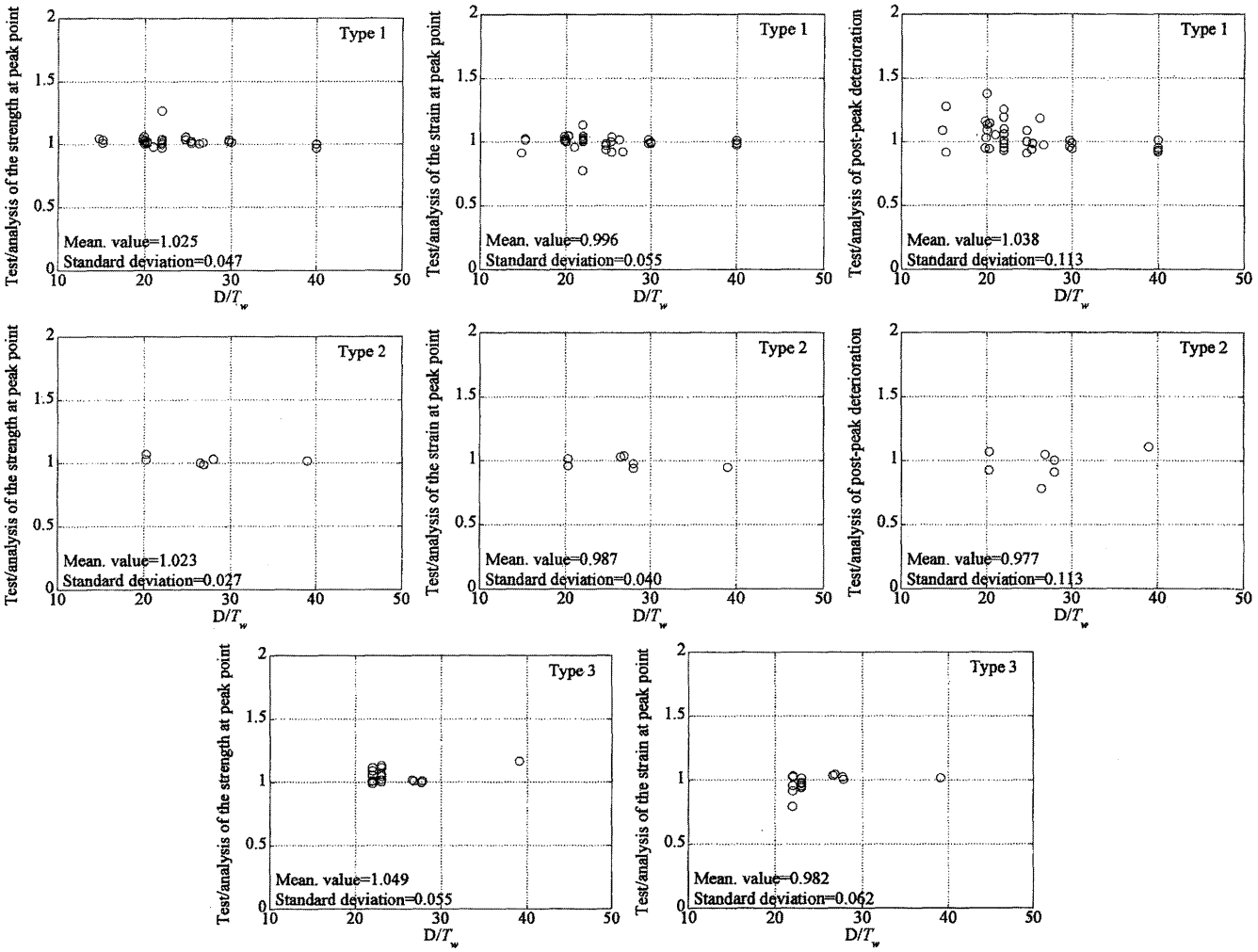

Fig. 10 Accuracy calibration of specimens with D/T_w (all data)

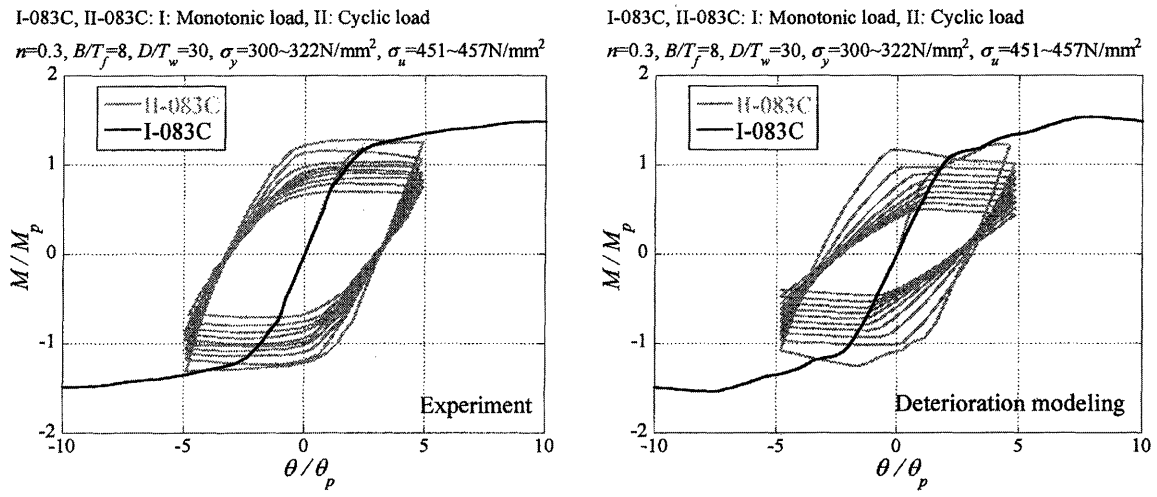

(a) Test results **(b) Analytical results**

Fig. 11 Cyclic deterioration of H-shaped steel component

Given that the strength and stiffness deterioration includes post-peak deterioration in skeleton curve under monotonic loadings (axial load, or horizontal load with constant axial load) and cyclic deterioration in hysteretic curve under cyclic loadings. Fig. 11 illustrates a typical example of the cyclic deterioration of H-shaped steel component under various loading histories. In Fig. 11, the post-peak deterioration in backbone curve and cyclic deterioration in hysteretic curve could be predicted by the deterioration model of H-shaped steel components.

Corresponding to H-shaped steel, for RC components, in addition to the above errors for calibration of steel components, the effect of material uncertainty (concrete, steel bars, H-shaped steel) also significantly influence the post-peak behavior. Unlike the components with only one type of local failure (local buckling), various types of local failure of RC components induced by different loading procedures are also a reason on larger deviation of calibrations.

4. CONCLUDING REMARKS

The deterioration modelling of RC and H-shaped steel components by incorporating the strength and stiffness deterioration is developed in this paper, in order to support the simulation of the collapse of high-rise buildings induced by local failure. Calibration of the deteriorating stress-strain models for RC and H-shaped steel components is based on comparisons between available experimental results and analytical results. Some results are concluded as follows.

(1) The constitutive model for reinforced concrete components incorporating local failure of concrete and buckling of steel bar validated by observed experiments, shows reliably accurate capability to predict the overall behaviour. Uncertainty of peak-point is rarely affected by loadings procedures, while, for post-peak deterioration, dispersion of uncertainty under cyclic loadings is distributed wider than that under axial loadings..

(2) For H-shaped steel, both peak point and post-peak deterioration can be simulated more accurately than RC components, due to the effect of mechanical behaviour of material and material composites.

Overall, uncertainty of the peak-point and post-peak deterioration shows various deviations, in which, post-peak deterioration is more difficult to be captured. The deterioration models for RC components and H-shaped steel components are expected to be utilized in the seismic response analysis of RC and steel high-rise moment-resisting frame buildings.

ACKNOWLEGEMENT

This study was financially supported by Grant-in-Aid for Scientific Research (B) No. 20360254 (Principal Investigator: Professor Uetani, Kyoto University). Beside, Prof. Araki from Kyoto University is also gratefully acknowledged for significant supports on this study.

NOTATION

B Width of section (mm)
C Effective length of hoop/stirrup reinforcement (mm)
D Length of section (mm)
D_c Width of hoop/stirrup reinforcement (mm)
E_c Younger's modulus of concrete (N/mm^2)
E_s Young's modulus of steel
$E_{s,\infty}$ Strain hardening modulus of steel
f'_c Compressive strength of plain concrete (N/mm^2)
f'_{cc} Compressive strength of confined concrete (N/mm^2)
L Longitudinal length of column (mm)
M Moment

M_p Full plastic moment
n Axial load ratio ($n=N_0/N_u$)
N_0 Axial force (kN)
N_u Full plastic axial force (kN)
p_w Hoop/stirrup ratio
r_{spm} Rate of the residual strength to the buckling strength
R_{ini} R (radian) for the first M&P skeleton curve
R_{II} R (radian) for the second M&P skeleton curve
S Spacing of hoop/stirrup reinforcement (mm)
T_f Flange thickness of H-shaped steel (mm)
T_w Web thickness of H-shaped steel (mm)
W Deterioration factor which is a function of f'_c and σ_{re}
V Normalized factor which is a function of E_c, σ_c and ε_c
α_f Normalized width-thickness ratio of steel flange
α_w Normalized width-thickness ratio of steel web
ϕ_w Nominal diameter of hoop/stirrup reinforcement (mm)
ρ_w Volumetric ratio of hoop/ stirrup reinforcement
λ Slenderness ratio of steel bar
σ_B Cylinder strength of concrete (N/mm^2)
σ_y Yield strength of steel (N/mm^2)
σ_{hs} Yield strength of hoop reinforcement (N/mm^2)
ε'_c Stain at the compressive strength of plain concrete
ε'_{cc} Stain at the compressive strength of confined concrete
ε_{lb} Strain at the local buckling of sectional steel (N/mm^2)
ε_{bu} Strain at the buckling of steel bar (N/mm^2)
τ Deterioration factor of confined concrete
τ_{lb} Deterioration modulus after (local) buckling of steel
τ_{lb2} Deterioration modulus at residual branch of steel
Δ Axial deformation (mm)
θ Rotation angle of components
θ_p Rotation capacity

REFERENCES

1) K. Uetani, H. Tagawa: Deformation Concentration Phenomena in the Process of Dynamic Collapse of Weak-Beam-Type Frames, J. Struct. Constr. Eng., AIJ, No. 483, pp. 51-60, 1996. (in Japanese)
2) D.C. Kent, R.Park: Flexural Members with Confined Concrete. Journal of Structural Division, ASCE, 97(7), PP. 1969–90, 1971
3) S. Popovics: A Numerical Approach to Complete Stress-Strain Curve of Concrete, Cement and Concrete Research, pp. 583-599, 1973.
4) S.A. Sheikh, S.M. Uzumeri: Analytical Model for Concrete Confinement in Tied Columns, Journal of Structural Engineering, ASCE, Vol.108, pp.2703-2722, 1982.
5) J. B. Mander, J. N. Priestly, R. Park: Theoretical Stress–Strain Model for Confined Concrete, Journal of Structural Engineering, ASCE, Vol. 114, No. 8, pp. 1804-26, 1988.
6) M. Sargin et al.: Effects of Lateral Reinforcement Upon the Strength and Deformation Properties of Concrete, Magazine of Concrete Research, Vol. 23, pp. 99-110, 1971
7) K. Sakino, YP. Sun: Stress-strain Curve of Concrete Confined by Rectilinear Hoop, J. Struct. Constr. Eng., AIJ, No. 461, pp. 95-104, 1994. 7 (in Japanese)
8) YT Bai, A. Kawano et al.: Constitutive Models for Hollow Steel Tubes and Concrete Filled Steel Tubes Considering the Strength Deterioration, J. Struct. Constr. Eng., AIJ, Vol. 77, No. 677, pp. 1141-1150, 2012.
9) A. Kawano, R.F. Warner: Nonlinear Analysis of the Time-Dependent Behaviour of Reinforced Concrete Frames, Research Report No. R125, Department of Civil and Environmental Engineering, The University of Adelaide, 1995.
10) W. Ramberg, W.R. Osgood: Description of Stress-Strain Curves by Three Parameters, Technical Note No. 902, National Advisory Committee For Aeronautics, Washington D.C., 1943.
11) M. Menegotto, P.E. Pinto: Method of Analysis for Cyclically Loaded RC Frames Including Changes in Geometry and Non-Elastic Behavior of Elements under Combined Normal Force and Bending, IABSE Congress Reports of the Working Commission Band, No. 13, 1973.
12) B. Kato, H. Akiyama, H. Yamanouchi: Experimental Law on Stress-Strain Curve of Steel Material, Summaries of Technical Papers of Annual Meeting Architectural Institute of Japan, AIJ, No. 48, pp.937-938, 1973. (in Japanese)
13) H. Akiyama, M. Takahashi: Influence of Bauschinger Effect on Seismic Resistance of Steel Structures, J. Struct. Constr. Eng., AIJ, No. 418, pp.49-57, 1990. (in Japanese)
14) Linghua Meng, K. Ohi, K. Yakanashi: A Simplified Model of Steel Structural Members with Strength Deterioration Used for Earthquake Response Analysis, J. Struct. Constr. Eng., AIJ, No. 437, pp.115-124, 1992. (in Japanese)
15) S. Yamada, H. Akiyama, H. Kuwamura: Deteriorating Behavior of Wide Flange Section Steel members in Post Buckling Range, J. Struct. Constr. Eng., AIJ, No. 454, pp.179-186, 1993. (in Japanese)
16) T. Nakatsuka, M. Maekawa, H. Nakagawa: Equations

to Estimate Strains at Buckling of Longitudinal Reinforcement Under Uniaxial and Monotonical Compression, Buckling of Longitudinal Reinforcement Arranged in Confined Concrete (Part 2), J. Struct. Constr. Eng., AIJ, No. 516, pp.145-149, 1999. (in Japanese)

17) K. Inoue, N. Shimizu, Plastic Collapse Load of Steel Braced Frames Subjected to Horizontal Force, J. Struct. Constr. Eng., AIJ, No. 388, pp. 59-69, 1988. 6 (in Japanese)

18) T. Suzuki et al.; Experiments on the Effects of Hoop Reinforcements in the Steel and R/C Composite, J. Struct. Constr. Eng., AIJ, No. 348, pp.61-74, 1985. (in Japanese)

19) D. Kato, Stress-Strain Behaviors of Square Confined Reinforced Concrete Columns, J. Struct. Constr. Eng., AIJ, No. 422, pp.65-74, 1991. (in Japanese)

20) Toneo Endo: An Experimental Study on Horizontal Force Failure of Reinforced Concrete Column Under Constant Axial force, Summaries of Technical Papers of Annual Meeting Architectural Institute of Japan, AIJ, No. 39, pp.227-230, 1968. (in Japanese)

21) J. Ishihara et al.: Seismic Behavior of Concrete Columns Made of High-Strength Materials Part 1 Outline of Experiments and Primary Results, AIJ Kyushu Chapter Architectural Research Meeting, No. 43, pp.425-428, 2004. (in Japanese)

22) S. Watson, R. Park: Simulated Seismic Load Test on Reinforced Concrete Columns, Journal of Structural Engineering ASCE, Vol. 120, No. 6, pp.1825-1849, 1994.

23) R. Park, M.J.N. Priestley, W.D. Gill: Ductility of Square-Confined Concrete Columns, Journal of the Structural Division, ASCE, Vol. 108, No. ST4, pp.929-950, 1982.

24) M.B. Atalay, J. Penzien: The Seismic Behaviour of Critical Regions of Reinforced Concrete Components as Influenced by Moment, Shear and Axial Force, Report No. EERC 75-19, University of California, Berkeley, Dec. 1975.

25) M.T. Soesianawati, R. Park, M.J.N. Priestley: Limited Ductility Design of Reinforced Concrete Columns, Report 86-10, Department of Civil Engineering, University of Canterbury, Christchurch, New Zealand, 1986.

26) H. Tanaka, R. Park: Effect of Lateral Confining Reinforcement on the Ductile Behaviour of Reinforced Concrete Columns, Report 90-2, Department of Civil Engineering, University of Canterbury, 1990.

27) S. Yamada et al.: Stub-Column Test Focused on Material Properties, (Part. 2 H-shaped Stub-Column Test), Summaries of Technical Papers of Annual Meeting Architectural Institute of Japan, AIJ, pp.1247-1248, 1992. (in Japanese)

28) M. Suzuki et al.: A Study on Interaction of Plate Elements of Structural Members Part 1 Outline and Stub-Column, Summaries of Technical Papers of Annual Meeting Architectural Institute of Japan, AIJ, pp.1339-1340, 1991. (in Japanese)

29) Mukai Akiyoshi et al.: Yield Ratio and Deformation Capacity of Steel Members 2. Stub Column Tests, Summaries of Technical Papers of Annual Meeting Architectural Institute of Japan, AIJ, pp.1239-1240, 1992. (in Japanese)

30) I. Mitani (1980), Study on Elasto-Plastic Behavior of Steel Members and Frames Subjected to Cyclic Loadings Considering Instability, Doctoral Dissertation, Kyushu University, Japan. (in Japanese)

31) Higashino Yoshiyuki et al.: Effects of the Value of the Yield Ratio of Steel on the Ductility of Steel Frame (Part. 1) Behavior of Steel Beam-Column, Summaries of Technical Papers of Annual Meeting Architectural Institute of Japan, AIJ, pp.1511-1512, 1991. (in Japanese)

（受理：平成24年6月7日）